CORROSION PERFORMANCE OF STRUCTURAL ALLOYS
IN COAL-COMBUSTION ENVIRONMENTS[*]

K. Natesan
Energy Technology Division
Argonne National Laboratory
Argonne, IL 60439

and

M. Freeman and M. Mathur
National Energy Technology Center
Pittsburgh, PA 15236

May 2000

DISCLAIMER

DISCLAIMER

Portions of this document may be illegible in electronic image products. Images are produced from the best available original document.

CORROSION PERFORMANCE OF STRUCTURAL ALLOYS
IN COAL-COMBUSTION ENVIRONMENTS[*]

K. Natesan
Energy Technology Division
Argonne National Laboratory
Argonne, IL 60439
and
M. Freeman and M. Mathur
National Energy Technology Center
Pittsburgh, PA 15236

ABSTRACT

Conceptual designs of advanced coal-fired combustion systems require high-temperature furnaces and heat transfer surfaces that operate at much higher temperatures than those in current coal-fired power plants. The combination of elevated temperatures and hostile combustion environments necessitates the development and application of ceramic materials in these designs. However, downstream of the combustion zone, a transition from ceramic to metallic materials will be required and the metallic components will experience much more elevated temperatures than those in current combustion systems. Furthermore, they will be subjected to combustion environments in which the deposit and gas chemistries could be different from those in current boiler systems. This paper discusses tests being conducted in a state-of-the-art, 0.5 MBtu/h pilot-scale facility to evaluate the corrosion performance of several candidate metallic materials. Alloys such as 800, 253 MA, 214, 625, 556, 617, 188, Alloy X, Fe aluminide, and MA 956 were exposed in the convective section of the facility at 650-1000°C. Results are presented on the chemistry and phases in the deposits and on the posttest examinations of the exposed specimens from the standpoint of scale type and thickness, internal penetration of the alloy, microstructural characteristics, and overall corrosion performance.

INTRODUCTION

Coal is a complex fuel that contains varying amounts of sulfur and a substantial fraction of noncombustible mineral constituents, commonly called ash. Conceptual designs of high-efficiency high-performance power systems that utilize coal as a feedstock require high-temperature furnaces and heat transfer surfaces capable of operating at higher temperatures than those used in conventional pulverized-coal-fired power plants.

The advanced concepts, as described in the U.S. Department of Energy Fossil Energy Vision 21 Program, would employ a combined cycle that uses a gas turbine driven by a working fluid (air) that is separately heated in a high-temperature advanced furnace, in addition to conventional steam turbines.[1] The high-temperature furnace in the advanced concept will heat air to an intermediate temperature of ≈1000°C and burn supplemental clean fuel to boost the temperature of air to the turbine inlet temperature of ≥1300°C. Use of supplemental fuel can be reduced as the materials and technology evolve to permit air to be heated to higher temperatures in the furnace. The high-temperature furnace represents a major departure from conventional pulverized-coal-fired boilers in which steam is raised to a maximum of only 530-620°C. The combination of elevated temperatures and hostile combustion environments in advanced concepts requires the use of ceramic materials in at least the first few passes of the heat exchangers in

these designs. For temperatures of 1100-1300°C, conventional metallic materials do not possess adequate strength properties and/or corrosion resistance for long-term service. However, a transition from ceramic to metallic material is anticipated for the heat-transfer surfaces in the area where the temperature in the system decreases from ≈1300 to 1000°C.

In addition, an important difference between the conventional boiler system and the advanced system is seen in the chemical and physical characteristics of the ash layers that can deposit on the heat transfer surfaces. Figure 1 is a schematic description of the deposits that can lead to corrosion of waterwall boiler tubes, steam superheaters, and air tubes during service in coal-fired systems. Fireside metal wastage in conventional coal-fired boilers can occur via gas-phase oxidation or deposit-induced liquid-phase corrosion. The former can be minimized by using materials that are oxidation-resistant at service temperatures of interest. On the other hand, deposit-induced corrosion of materials is an accelerated type of attack influenced by the vaporization and condensation of small amounts of impurities such as sodium, potassium, sulfur, chlorine, and vanadium, or their compounds that are present in the coal feedstock.

The deposits that form on the air tubes are likely to be dominated by alkali sulfates and coal slags in the advanced system rather than by pyrosulfates or alkali-iron-trisulfates, which form on the boiler waterwall and steam superheater materials. A major concern is the long-term performance of the air tubes because of the increased mobility of corrosion-accelerating agents in the deposit layers due to the much higher temperature of the heat transfer surfaces in the advanced system. A major challenge is to develop methods to combat severe deposition, erosion, and corrosion (DEC) of heat transfer surfaces exposed to higher-than-normal temperatures. These methods could include fuel selection, cleaning of aggressive contaminants from coal, fine grinding of coal, use of additives, and selection of advanced corrosion-resistant ceramic materials, coatings, and advanced alloys for vulnerable heat transfer sections. A discussion of the corrosion mechanisms and performance of materials for boiler waterwall and steam superheaters is presented in Ref. 2.

The objectives of the present program are to (a) evaluate the chemistry of gaseous and condensed products that arise in combustion of coal; (b) evaluate the corrosion performance of
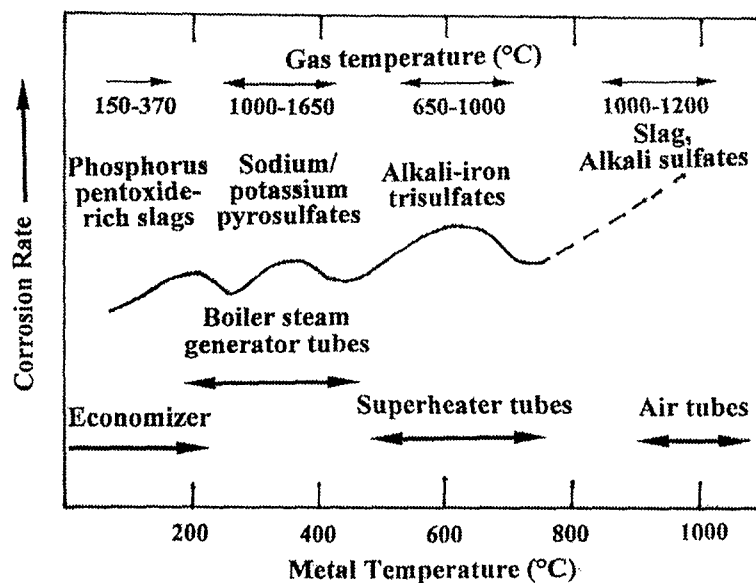

Figure 1. Regimes of fireside corrosion in coal-fired boilers

candidate materials in laboratory experiments conducted in simulated combustion environments, including deposits; and (c) expose candidate alloys and coatings in large-scale coal-burning combustion facilities and evaluate their corrosion performance. This work addresses the corrosion performance of materials intended for air-tube applications at elevated temperatures where the potential deposits are ash constituents transformed into slag and alkali sulfates.

Chemistry calculations determine the types and amounts of combustion products over the wide temperature range of 700-1700°C and at 1 atm pressure. The experimental program on heat exchanger materials will develop mechanistic information on the roles of material composition, ash constituents, combustion deposits, chlorine, alkali sulfates, and sulfur sorbents in the corrosion process. The program emphasizes corrosion evaluation of materials in the presence of coal/ash environments at temperatures between 650 and 1100°C. Coal/ash chemistries synthesized on the basis of thermodynamic/kinetic calculations, together with slags from actual combustors, are used in the laboratory program. The paper presents information on the chemistry of and mineralogical phases in deposits and corrosion (scaling and penetration) test results for several metallic materials that were exposed during three runs in the pilot-scale facility.

MATERIALS AND EXPERIMENTAL PROCEDURE

Several alloys, both ASME coded and uncoded materials selected on the basis of their high creep strength at elevated temperatures, were used in the study to evaluate their corrosion resistance; their chemical compositions are listed in Table 1. Among those selected, alloys 800HT, 310 stainless steel, 253MA, 556, MA956, and FAL are all iron-base alloys. All except FAL contained Cr in a range of 21-25 wt.%. MA956 is an oxide-dispersion-strengthened alloy, whereas FAL is an intermetallic Fe aluminide alloy. Among the six alloys, the first four are chromia formers and the last two are alumina formers. The second set of alloys X, 625, 617, 214, and 671 are all Ni-base alloys whose Cr contents ranged from 16 to 48 wt.%. All except 214 are chromia formers. Alloy 214, containing 16 wt.% Cr and 4.5 wt.% Al, is an alumina-forming alloy. Alloy 188 is Co base, contained 22 wt.% Cr, and is a chromia former.

The alloys were tested by exposing flat coupon specimens in the Combustion and Environmental Research Facility (CERF) at the Pittsburgh site of the National Energy Technology Laboratory (NETL). The CERF is a state-of-the-art, 0.5-million-Btu/h pilot-scale facility designed to conduct a wide range of combustion and pollution control studies of most solid, liquid, and gaseous fuels and to achieve similarity with full-scale utility and industrial boilers. The CERF is designed to

Table 1. Nominal chemical compositions (wt.%) of alloys selected for study

Material	C	Cr	Ni	Co	Mn	Si	Mo	Al	Fe	Other
800HT	0.08	21	32.5	-	1.0	0.5	-	0.5	Bal[a]	Ti 0.5
310	0.08	25	20	-	1.2	0.5	-	-	Bal[a]	
253MA	0.10	21	10.9	-	0.3	1.8	-	-	Bal[a]	Ce 0.03
556	0.10	22	20	20	1.0	0.4	3.0	0.2	Bal[a]	W 2.5, Ta 0.6
MA 956	0.05	20	-	-	-	-	-	4.5	Bal[a]	Y$_2$O$_3$ 0.5
FAL	-	5.5	-	-	-	-	-	15.9	Bal[a]	Zr 0.1, B 0.05
X	0.1	22	Bal[a]	-	0.5	0.5	9.0	-	18.5	Co 1.5, W 0.6
625	0.05	22	Bal[a]	-	0.3	0.3	9.0	0.2	2.5	Nb 3.7, Ti 0.2
617	0.07	22	Bal[a]	12.5	0.6	0.5	9.0	1.2	2.5	Ti 0.4
214	-	16	Bal[a]	-	-	-	0.5	4.5	2.5	Co 2.0, W 0.5
671	0.05	48	Bal[a]	-	-	-	-	-	-	Ti 0.35
188	-	22	22	Bal[a]	-	-	-	-	3.0	W 14, La 0.07

[a]Indicates balance.

closely duplicate typical full-scale specifications for:

- Solid fuel fineness or liquid fuel atomization quality.
- Burner relative mass flow (fuel and air) and velocities.
- Furnace temperature distributions.
- Radiant furnace residence time.
- Convective-section gas velocity.

Material exposures in CERF are conducted in a piggyback mode, whereby normal CERF testing proceeds in terms of evaluating combustion of various coals, coal blends, and cofiring with biomass. With this approach, comparative assessments of many materials at different locations could be made economically before pursuing dedicated-materials CERF tests that would require continuous operation of the facility for 500 h or more. Coupon samples of several of the metallic materials (see list in Table 1) were mounted with ceramic spacers on a high-temperature materials testing probe. Three runs were conducted in the test facility, and the details are listed in Table 2 on the time of combustion and feedstocks used during the runs.

In Run 1, the specimens were exposed for a total time of 754 h, of which solid feed was used

Table 2. Feedstocks and run times used during alloy exposure in CERF

	Main coal	Secondary coal	Other fuel	Main coal	Sec. coal	Natural gas	Other fuel	Total time (h)
Run 1	Pittsburgh	-	-	62	-	43	-	105
	Pittsburgh	E. Kentucky	-	33	20	44	-	97
	Pittsburgh	-	-	61	-	33	-	94
	Pittsburgh	PA anthracite	-	25	27	43	-	95
	Pittsburgh	-	-	29	-	70	-	99
	Pittsburgh	E. Kentucky	Switchgrass Illinois No. 6 PA anthracite	16	10	29	29	84
	Pittsburgh	-	-	61	-	30	-	91
	Pittsburgh	Illinois No. 6	Kathara middlings PA anthracite	42	9	30	8	89
			Total: 754 h; Solid feed: 432 h					
Run 2	Western Arctic	-	-	32	-	60	-	92
	Western Arctic	-	-	68	-	15	-	83
			Total: 175 h; Solid feed: 100 h					
Run 3	Pittsburgh	-	-	73	-	28	-	101
	Pittsburgh	-	Hybrid willow 15%	5	-	73	9	87
	Illinois No. 6	-	-	8	-	422		430
	Pittsburgh	-	Pallet 15% Paper 10%	41	-	53	8	102
	Pittsburgh	-	Pallet 15% Pine bark 5-25% Switchgrass 15%	1	-	61	38	100
	E. Kentucky	Illinois No. 6	Wyoming coal	55	20	13	17	105
	Pittsburgh	-	Paper 8%	1	-	55	29	85
	Pittsburgh	-	Switchgrass	26	-	35	38	99
	Pittsburgh	-	Sawdust Switchgrass	43	-	44	7	94
			Total: 1203 h; Solid feed: 419 h					

Column group header: "Test time (h) on" spans Main coal, Sec. coal, Natural gas, Other fuel.

for 432 h. The feedstock in Run 1 was predominantly coal and the specimen temperatures ranged from 870 to 1000°C. In Run 2, the specimens were exposed for a total of 175 h, of which the time for solid feed was 100 h. The feedstock in Run 2 was Western arctic coal and the specimen temperature was 650°C. In Run 3, the specimens were exposed for a total of 1203 h, of which the time for solid feed was 419 h. The feedstock in Run 3 was predominantly coal, but biomass was combusted for 146 h and the specimen temperature ranged between 870 and 982°C. It should be noted that coal and natural gas were used in the initial stages of each sub-run (see listing in Table 2), and biomass was combusted during the later stages of each sub-run. Therefore, the deposit adjacent to the specimens consisted of predominantly coal-derived ash/slag components, while biomass ingredients were generally present on the gas side of the deposit.

RESULTS AND DISCUSSION

DEPOSIT CHARACTERISTICS

Thermodynamic calculations were used to evaluate the chemistries of gaseous and condensed phases that occur during combustion of an Illinois bituminous coal. The computer program used for the calculations is based on calculating the equilibrium concentrations of various species by minimizing the free energy of the system. Details of the calculations are presented in Ref. 3. Calculated results for the chemistry of condensed phases and the gaseous phase at the combustion air:coal stoichiometric ratio of 1.3 showed that coal combustion results in a liquid phase that is essentially a silica-saturated silicate and/or sulfate condensate, with the components made up largely of SiO_2, Al_2O_3, CaO, Fe_2O_3, Na_2SO_4, and $NaCl$ (see Fig. 2). At temperatures below 1180°C, the partial pressures of $NaCl(g)$, $HCl(g)$, $NaOH(g)$, and $Na(g)$ change abruptly; a complex sodium aluminosilicate, $Na_2O \cdot Al_2O_3 \cdot 6SiO_2(s)$, tends to form; and the liquid silicate-sulfate condensate disappears. Formation of the complex silicate requires intimate contact among several gaseous and condensed phases, but the probability of such contact in real systems is expected to be low. Under nonequilibrium conditions, where such reactions are constrained, stability of the liquid sulfate-silicate condensate extends to temperatures as low as 890°C.

Based on the results of these calculations, the general behavior of the solution phase under oxidizing conditions can be described as follows. A liquid solution phase, consisting mostly of silicates of aluminum, calcium, sodium, magnesium, and iron, is present at 1730°C. The mole fraction of
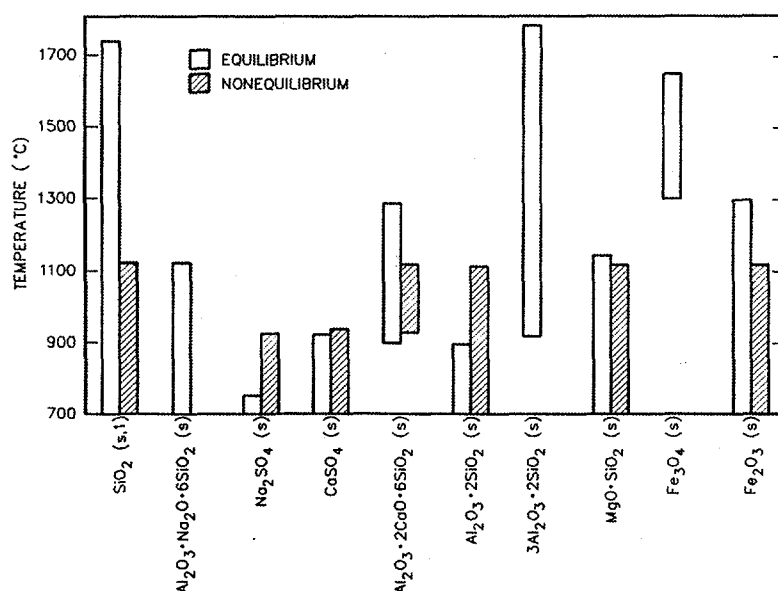

Fig. 2. Approximate temperature ranges for stability of condensed phases during combustion of high-sulfur coal with 30% excess oxygen.

Na$_2$SO$_4$ phase in the liquid is <0.01 above 1280°C. The concentration of Na$_2$SO$_4$ rises rapidly as the temperature decreases and becomes a major component of the solution at 980°C. The mole fraction of Na$_2$SO$_4$ may increase to 0.9 or more at 980°C. However, these are thermodynamic calculations and indicate only the stability of different phases that can form at various temperatures. The formation of a specific phase in practice will be strongly dictated by the kinetics; furthermore, the deposit can have a wide variation in composition and stratification of various phases, and this can also influence the corrosion performance of the underlying metal alloy. Chemistry calculations on the anticipated phases in deposits at temperatures of interest for air tubes showed mullite, Ca aluminosilicates, silica, and iron oxide when U.S. eastern coals are combusted under excess air conditions.

Deposits accumulated on several specimens exposed in Runs 1-3 were analyzed by X-ray diffraction. The results indicated that deposits from Runs 1 and 3 consisted of mullite (3Al$_2$O$_3$·2SiO$_2$), hematite (Fe$_2$O$_3$), and anorthite (CaO·Al$_2$O$_3$·2SiO$_2$). In Run 2, the deposits consisted of silica (SiO$_2$), wollastonite (CaSiO$_3$), microcline (KAlSi$_3$O$_8$), and trace of arcanite (K$_2$SO$_4$). Combustion of biomass in Run 3 (when compared with predominantly coal-only combustion in Run 1) did not result in deposits high in alkali or phosphorus. In Run 3, coal and natural gas were always combusted in the early stages, and biomass was cofired in the later stages; therefore, the deposits adjacent to the metal sample will consist of ash components and the biomass constituents will be present on the gas side of the deposit and are not expected to accelerate corrosion of the metallic alloys in the present runs. The observed deposits also indicate that the liquidus temperature of most of the phases (except K$_2$SO$_4$) are 1500-1850°C and that reactions between coal ash deposit and the metallic alloys occur predominantly in the solid state.

CORROSION PERFORMANCE

To examine the corrosion performance of metallic alloys, the exposed specimens were analyzed in detail by scanning electron microscopy (SEM) and energy-dispersive X-ray (EDX) analysis to evaluate the scale composition and the thickness and depth of internal penetration into the substrate. Figure 3 shows macrophotographs of specimen assemblies and layouts of specimens exposed in Runs 1-3 in CERF. Figures 4 and 5 contain SEM photomicrographs of cross sections of Fe- and Ni-base alloys, respectively, after exposure in Run 1. Similar evaluation was conducted on specimens exposed in Runs 2 and 3. The exposure temperatures for specimens in Runs 1, 2, and 3 were 870-1000, 650, and 870-980°C, respectively. In general, the Fe-base wrought alloys such as 800HT, 310 stainless steel, and 556 developed Cr oxide or (Cr,Fe)oxide, whereas MA956 and FAL alloys developed thin alumina scales. The Ni-base alloys generally developed Cr oxide scales; alloy 214, which contains 4.5 wt.% Al, developed an alumina scale. The Co-base alloy developed (Fe,Cr,W)oxide.

In specimens exposed in Run 1, scale thickness ranged from 3 to 5 μm in alumina-forming alloys and from 5 to 25 μm in chromia-forming alloys. Several alloys exhibited significant penetration, largely determined by the alloy composition rather than by the protectiveness of the scale. For example, alloys such as 214 (with 4.5 wt.% Al), 617 (1.2 wt.% Al), 556 (0.2 wt.% Al and 0.6 wt.% Ta), and 800HT (0.5 wt.% Al and 0.5 wt.% Ti) exhibited significant internal oxidation along grain boundaries in the substrate. The morphological features of the scales and internal penetration in specimens exposed in Run 3 were similar to those observed for specimens exposed in Run 1. The specimens exposed in Run 2 were at a lower temperature and for a shorter time; as a result, the scales were predominantly mixed oxides of (Cr,Fe)oxide, (Cr,Al)oxide, or (Cr,Si)oxide, and penetration of the alloys was minimal. Scale thicknesses in MA956 and FAL alloys exposed in Run 3 were somewhat greater than those observed in Runs 1 and 3, because at the lower temperature of 650°C, γ-alumina (with a higher growth rate) probably forms, whereas at 870-1000°C (in Runs 1 and 3) α-alumina (with a slower growth rate) is expected.

The data on scale thickness and internal penetration for several alloys from various runs were normalized assuming a parabolic kinetics, and comparative plots were developed to assess the corrosion performance of various alloys. Figure 6 shows the scaling- and penetration-rate data obtained for all of the alloys exposed in Runs 1, 2, and 3 in the CERF. Based on this study, the corrosion rates (scaling plus penetration) for Fe- and Ni-base alloys are ≈0.3 and 0.15-0.40 mm/y, respectively. The results indicate that
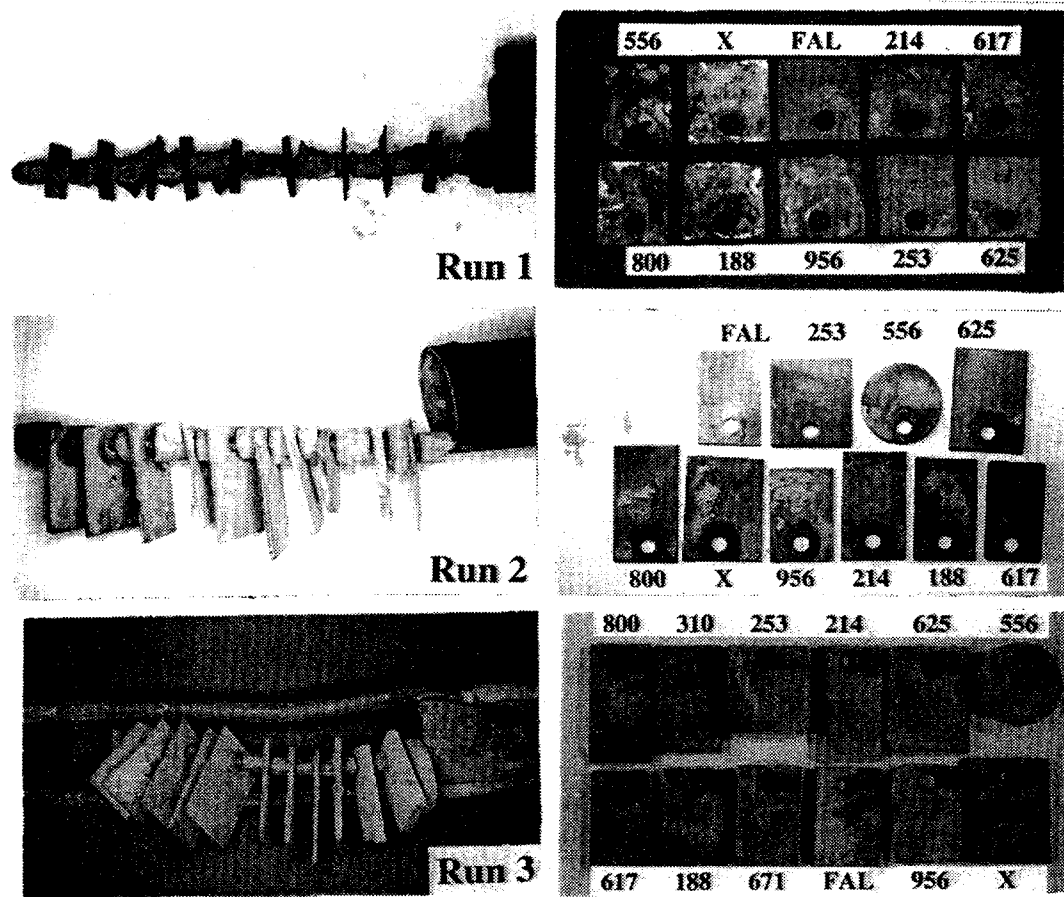
Figure 3. Macrophotographs of coupon specimens exposed in Runs 1, 2, and 3 in convective pass section of CERF.
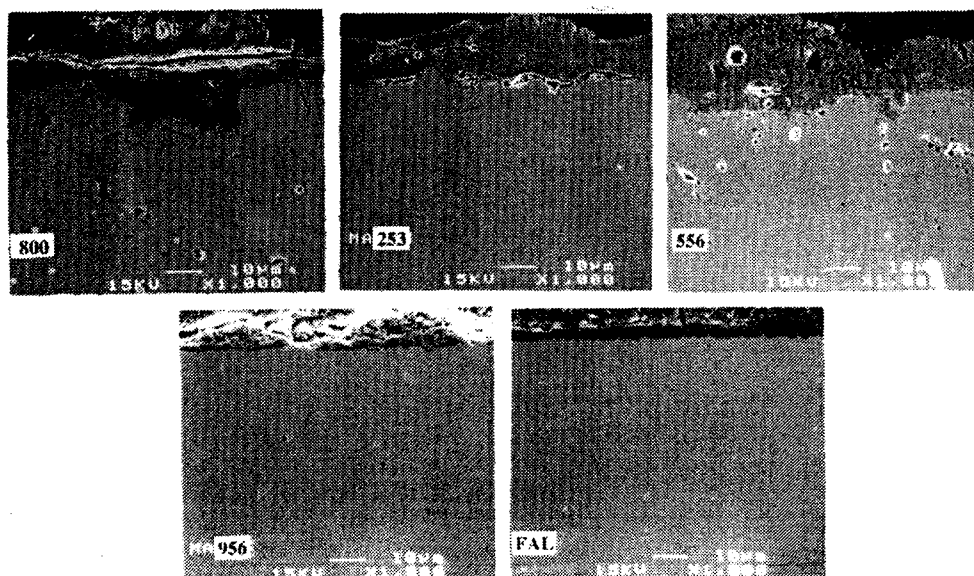

Figure 4. SEM microphotographs of coupon specimens of Fe-base alloys exposed in Run 1 in convective pass section of CERF.
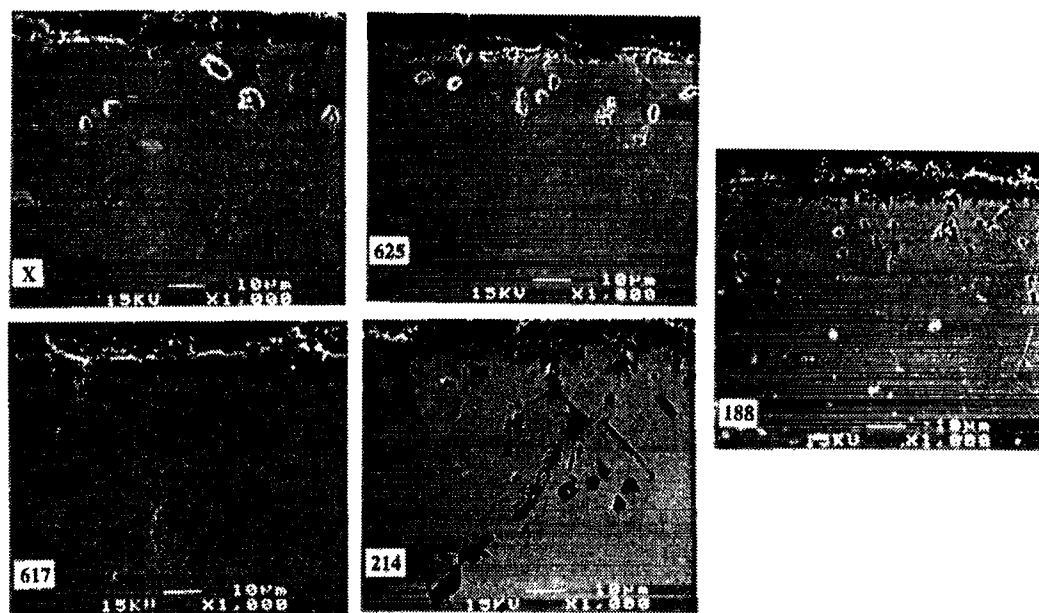
Figure 5. SEM microphotographs of coupon specimens of Ni-base alloys exposed in Run 1 in convective pass section of CERF.
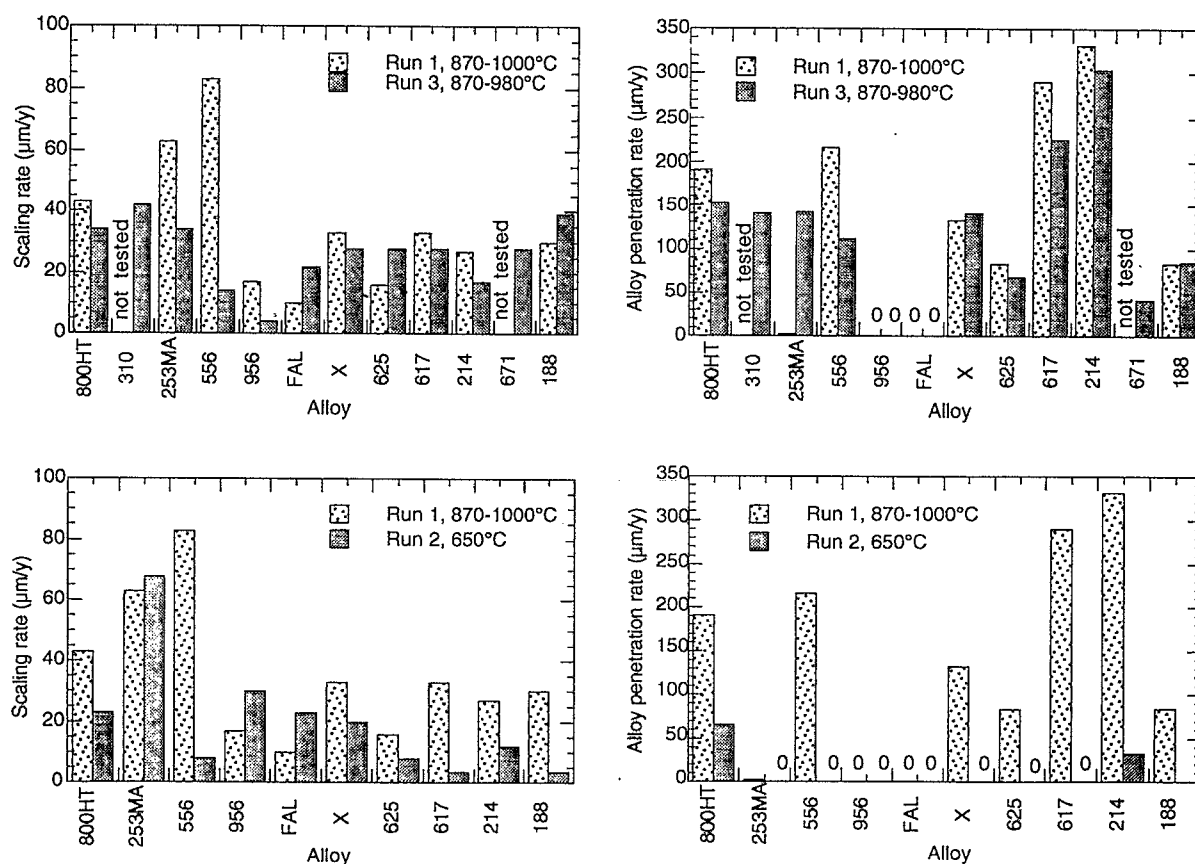

Figure 6. Comparative scaling- and penetration-rate data for alloys exposed in Runs 1, 2, and 3 in CERF.

in the case of air tubes with 5 to 6 mm wall thickness, these corrosion rates will lead to a thickness loss (based on parabolic kinetics) of 1 mm for Fe-base alloys and 0.5-1.25 mm for Ni-base alloys after 10 years of service at temperatures of 900 to 1000°C.

SUMMARY

We have conducted three tests by exposing several candidate metallic alloys in coal/biomass combustion environments in NETL's Combustion and Environmental Research Facility (CERF). The specimens were exposed in the convective section at temperatures of 650 and 870-1000°C for times of up to 1200 h. X-ray diffraction analyses of deposits collected on exposed specimens showed mullite, hematite, and anorthite phases in Runs 1 and 3, and silica, wollastonite, and microcline in Run 2. All of these phases have melting temperatures of >1500°C and therefore, the deposit/alloy interactions occur via solid-state mechanisms at the temperatures of interest (900-1100°C) for air tubes in advanced combustion systems. Scale thickness and depth of internal penetration were measured on all exposed specimens by scanning electron microscopy. Based on this study, the corrosion rates (scaling plus penetration) for Fe- and Ni-base alloys are ≈0.3 and 0.15-0.40 mm/y, respectively, at temperatures of up to 1000°C. These corrosion rates will lead to a thickness loss (based on parabolic kinetics) of 1 mm for Fe-base alloys and 0.5-1.25 mm for Ni-base alloys after 10 years of service at temperatures of 900 to 1000°C.

REFERENCES

1. G. Rudins and R. A. Bajura, U.S. Department of Energy, Fossil Energy, Vision 21 Program, 1999.

2. K. Natesan, Journal of Metals, 43 (11), p. 61, 1991.

3. S. N. Sinha, K. Natesan, and M. Blander, "Chemistry of Gaseous and Condensed Products in Coal Combustion and Conversion Systems," Argonne National Laboratory Report ANL-89/25, 1989.